Perumal Senthil Kumar (Orcid ID: 0000-0002-3649-9144)
Raghukanth S.T.G. (Orcid ID: 0000-0002-8344-797X)
Dhabu Anjali C (Orcid ID: 0000-0002-2913-3013)

The seismically active lobate scarps and co-seismic lunar boulder avalanches triggered by 3rd January 1975 (M_W 4.1) shallow moonquake

P. Senthil Kumar[1*], Rupali Mohanty[1], K. Jaya Prasanna Lakshmi[1], S.T.G. Raghukanth[2], Anjali C. Dhabu[2], R.P. Rajasekhar[3], and Rajeev Menon[1]

[1]CSIR-National Geophysical Research Institute, Hyderabad, India
[2]Indian Institute of Technology – Madras, Chennai, India
[3]ISRO-Space Applications Centre, Ahmedabad, India

*Corresponding author: senthil@ngri.res.in; senthilngri@yahoo.com

Key Points

- A set of lobate scarps responsible for the 3rd January 1975 shallow moonquake (M_W 4.1) has been detected in Laue crater floor
- Co-seismic boulder avalanches of different ages have been identified on the interior walls of impact craters near the epicenter

Fault slip along the Lorentz basin wall beneath Laue crater floor produced the lobate scarps and shallow moonquakes **Keywords:**

Shallow moonquake; Lobate scarps; Boulder falls; Recent seismicity; Seismic ground motion; Seismo-tectonics

Abstract

On January 3, 1975, the largest shallow moonquake (M_W 4.1) occurred at Laue impact crater on the Moon. The fault responsible for the moonquake and origins of co-seismic boulder avalanches are unknown. Our study reveals a set of previously unreported, seismically active, young lobate scarps near the epicenter. In addition, hundreds of boulder falls are observed on the interior walls of two impact craters on either side of the lobate scarps. The varying preservation levels and crater size-frequency distributions of impact craters superimposed on the boulder falls indicate their episodic origins at 1.6 Ma and during the 1975 shallow moonquake. Our ground motion simulations confirm that the M_W 4.1 moonquake along the lobate scarp at 1-5 km focal depths produced strong ground shaking that triggered the boulder avalanches. Also, the fault slip along the Lorentz basin wall beneath the Laue crater floor produced the lobate scarps and the shallow moonquakes.

Plain Language Summary

Like Earth, the Moon is also seismically active but with relatively lesser intensity. The seismometers installed by the Apollo missions detected 28 shallow moonquakes during 1969-1977. The moonquake that occurred at Laue crater on 3rd January 1975 is the largest recorded moonquake (M_W 4.1). Our analysis of high-resolution satellite images and topographic data obtained by NASA's Lunar Reconnaissance Orbiter mission aided in the discovery of a set of young lobate scarps near the epicenter and its genetic link to the 1975 moonquake. The moonquake also generated strong ground motion around the epicenter and triggered formation of co-seismic boulder avalanches on the interior walls of near-by impact craters. We also found that boulder avalanches were formed during an earlier episode of seismic activity at 1.6 Ma. Furthermore, we deduce that the lobate scarps at Laue crater were formed in response to the reactivation of the basin wall normal fault of Lorentz peak-ring basin. Our study indicates that the lobate scarps in Laue crater are seismically active and their seismic activity could be further studied during future landing missions.

1. Introduction

The Moon is the only body in our solar system next to Earth, where the moonquakes were instrumentally recorded by a network of seismometers, although the seismic activity of Mars is currently monitored by NASA's InSight mission and the results are awaited. The passive seismic network installed by the astronauts at the Apollo 12, 14, 15 and 16 landing sites on the moon detected a set of 28 shallow moonquakes during 1969-1977 and these quakes resemble the terrestrial intra-plate earthquakes (Nakamura et al., 1979; Nakamura, 1980). Of these moonquakes, the event that occurred on 3rd January 1975 is the largest in terms of seismic moment magnitude (M_W~ 4.1) and stress drop (~210 MPa) (Oberst et al., 1987). The epicentral location of this event was fixed at 29°N and 98°W with a location error of 1 degree (~32 km) (Nakamura et al., 1979). It falls on the north-western interior wall of the 92-km-diameter Laue crater that overlies the 351-km-diameter Lorentz peak ring basin (**Figure 1**). The tectonic structures (e.g., faults) responsible for this moonquake are unknown. By virtue of being the largest recorded moonquake, it should have generated strong ground motion around the epicenter, which may have led to the formation of co-seismic mass wasting features (e.g., boulder falls) on near-by steep slopes (e.g., impact crater interior walls). In order to identify the seismogenic fault and the formation of co-seismic boulder falls, we have carried out a detailed study of Laue crater and the surrounding regions including Lorentz basin, using the NASA's Lunar Reconnaissance Orbiter (LRO) mission data. Our study provides new evidence of lobate scarps near the 1975 shallow moonquake epicenter and hundreds of boulder falls on the interior walls of two nearby impact craters. Hence, we present: (1) the nature of the lobate scarps and their morphological properties, (2) morphology of the boulder falls and their stratigraphic relations and the model formation ages, (3) numerical simulation studies for understanding the nature of shallow moonquake

ground motion and its role in the formation of boulder falls on the interior walls of impact craters, and (4) calculation of impact seismicity from the recent impact events to rule impacts out as a source. Finally, we discuss the genetic relation between the lobate scarps and the basin wall structure of Lorentz peak-ring basin.

2. The Study Area

Laue crater is a 92 km-diameter and 2.4 to 5.1 km deep complex impact crater (**Figure 1b**). It has an elongated central peak roughly in an E-W direction, with a length of ~18 km and a maximum width of ~10 km. Many smaller simple impact craters (bowl-shaped) of varying diameters are superimposed on Laue crater. Of these,we found two impact craters (craters 1 and 2) containing the boulder falls on their interior walls (**Figure 1b**). Crater 1 is a 9 km wide and 1.8 km deep simple crater, located to the north of central peak. Crater 2 is a 8.8 km wide and 1.92 km deep simple crater emplaced on the southwestern rim of Laue crater. We report previously unreported lobate scarps located on the Laue crater floor, to the west of the central peak (**Figure 1a**). Lorentz basin (**Figure 1a**) is a peak ring basin with a basin diameter of 351 km and peak ring diameter of 173 km (Baker et al., 2012). It is located about 1600 km north of Orientale basin and about 170 km west of Oceanus Procellarum.

3. Data and Methods

We used three data sets from the three LRO instruments: (1) 0.5-m-per-pixel LROC Narrow Angle Camera (NAC) panchromatic images for characterizing the lobate scarps and boulder falls; (2) 100-m-per-pixel LROC Wide Angle Camera (WAC) image mosaic for studying the regional geologic context of the study area (Robinson et al., 2010); and (3) 256-pixels-per-

degree LOLA (e.g., Smith et al., 2010) and 512-pixels-per-degree merged Kaguya-LOLA topographic data (Baker et al., 2016) for morphometric analysis. We have utilized ArcGIS desktop 10.0 software for digital geological mapping and analysis. Using the ArcGIS 3-D Analyst tool, we obtained the topographic profiles of the boulder fall sites from the integrated digital terrain model that incorporates both LOLA and higher resolution Kaguya topographic data. For analysing the gravity signatures and crustal thickness variation in the study area, we used Gravity Recovery and Interior Laboratory (GRAIL) mission data (**Supplementary Materials**).

4. Results

4.1. Lobate Scarps

A 25-km-long and 5-km-wide NNW-SSE zone containing a set of previously unreported lobate scarps is found between the western rim and the central peak of Laue crater (**Figure 1**). It consists of nineteen individual lobate scarps of varying lengths, from 0.3 to 11.2 km (**Figure 2a** and **Figure S1**), occurring within 1° location-error circle of the 3rd January 1975 moonquake epicenter given by Nakamura et al. (1979). A majority of scarps are roughly oriented in NW-SE to NNW-SSE directions, while a few minor ones are in E-W to NE-SW directions (**Figure 2a**). The scarps in general occur in the form of anastomosing left-steps. The scarps exhibit linear to curvilinear trends with surface expression of lobate topographic rises; the steep sides of scarps face the vergence (or movement) directions, while the gently sloping back limbs face the opposite direction (**Figures 2b-2g**). Some scarps exhibit crisp surface ruptures (**Figures 2d and 2e**). Geometries of most scarps are influenced by the southerly vergence of the underlying thrust faults (**Figures 2b and 2c**), although some

segments exhibit northerly vergence as seen in scarps 2, 4 and 5 (**Figures 2d-2g**). In **Figures 2d and 2e**, two parallel scarps exhibit opposite vergence directions: the northern and southern scarps respectively have northerly and southerly vergence directions. They imply two oppositely dipping thrust faults merging underneath at some depth, thus defining a flower structure. Presence of small and fresh cross-cut impact craters and superimposed impact craters on the scarps suggests that they are young thrust faults (e.g., Watters et al., 2010; Kumar et al., 2016). For example, the south-eastern rim of a 90 m diameter fresh impact crater is deformed by a northerly verging scarp is clearly seen in **Figures 2f and 2g**. Some surface ruptures do not have superimposed impact craters, indicating their possible recent origins.

The lobate scarps in the Laue crater floor are the most likely seismogenic source of the 3rd January 1975 moonquake, given their location falling within the moonquake's location error-circle. Hence, we relocated the 3rd January 1975 moonquake epicenter given by Nakamura et al. (1979) to the largest lobate scarp segment (**Figure 1b**), although it may have potentially originated along any one of the scarp segments.

4.2. GRAIL Gravity and Crustal Thickness

Laue crater is superimposed on the Lorentz basin rim and postdates it (**Figure 1)**. Hence, the trace of Lorentz basin wall should be buried beneath the Laue crater floor. Interestingly, the location of lobate scarps coincides with the buried basin wall (**Figures 1a and 1b**). In order to confirm the trace of Lorentz basin wall beneath the Laue crater floor, we analysed the GRAIL gravity data as they would shed light on the sub-surface structures pertaining to the lunar impact craters and basins (e.g., Neumann et al., 2015). The gravity data analysis is

given in the **supplementary materials**. **Figure 1c and 1d** show the residual Bouguer gravity anomaly and crustal thickness map of Laue crater region, respectively. The residual Bouguer gravity map (**Figure 1c**) clearly shows the gravity anomaly of Lorentz basin wall on either side of Laue crater passing through the Laue crater floor, thus confirming the presence of Lorentz basin wall beneath the Laue crater floor (**Figure S2**). Crustal thickness of Laue crater region varies from 36 km to 42 km (**Figure 1d**). Crustal thickness variation along the two profiles across the lobate scarps zone (**Figure S3**) shows the crust beneath the lobate scarp is thinner than the adjacent floor and crater wall. The crustal thinning at the lobate scarp zone is attributed to the presence of Lorentz basin wall fault.

4.3. Boulder Avalanches

It is well understood that boulder falls provide important insights into moonquake ground motion (e.g., Kumar et al., 2016). Within 25-35 km radius from the relocated epicenter, we found several hundred boulder falls on the interior walls of two impact craters (craters 1 and 2, hereafter) on either side of the scarp zone (**Figures 1b and 3**). The transport of boulders on the crater wall produced trails exhibiting sliding, rolling and bouncing marks, and the source boulders that produced the trails are found at the terminus. At many places, the trail marks have disappeared while the source boulders are still present. Hence, the boulders are of two types – with or without associated boulder trails. In many cases, the trails are very fresh, while some exhibit varying levels of degradation. The older trails display pronounced degradation than the younger trails. The trails also exhibit cross-cutting relations: the fresh trails are superimposed on the degraded trails, indicating their younger ages (**Figure 3a**).

The boulder falls containing trails can be classified into two age types (**Figure 3a**). A set of boulder trails without superimposed fresh impact craters on them is identified as younger boulder falls (first set); they also have fresh appearance and cross-cut small fresh impact craters (**Figure 3a**). The other set of boulder trails with superimposed impact craters on them is classified as older boulder falls (second set). The boulders without trails (third set) should have been formed before the first and second sets of boulder falls. We have mapped 435 prominent boulder trails in crater 1 and out of which 304 trails belong to the younger generation (**Figures 3b-c**; **Figure S4**). At crater 2, we identified 136 older falls and 256 younger falls (**Figures 3d-e; Figure S4**). We also measured the size and aspect ratio (width/length) of the source boulders associated with the trails. The boulders at crater 1 have an average diameter of 3.11 m and aspect ratio of 0.78. Similarly, the boulders at crater 2 have an average diameter 3.01 m and aspect ratio of 0.79.

In general, the boulder trails occur on gentle crater wall slopes with an average slope of 26 degrees (**Figure S5**), while their boulder source regions are ~2-4 degrees steeper than the trail regions (**Figure S5**). The run-out efficiency (a ratio between the horizontal distance travelled by the boulder and the vertical fall height) of most boulder trails is greater than 1.7 (**Figure S6**), implying the requirement of some triggering mechanisms (ground shaking from moonquake or impact) for their origins (Howard, 1973; Iverson, 1997; Kumar et al., 2016). The slope properties of boulder falls at craters 1 and 2 are similar to those of Schrödinger basin (Kumar et al., 2016), where the shallow moonquake triggered boulder falls has been reported near the seismically active lobate scarps.

4.4. Ages of Boulder Falls

Among three sets of boulder falls, the second set containing superimposed impact craters on the trails (older boulder falls in **Figures 3b and 3d**) permit us in dating their absolute model formation ages using the conventional crater counting method (Neukum et al., 2001). The superimposed craters emplaced on the trails in a given area were counted using the *CraterTools* software (Kneissl et al., 2011); it provided a spatial crater-count file (SCC file), which was used for the statistical analysis utilizing the *Craterstats* software (Version 2.0) of Michael and Neukum (2010). The model formation age of a group of boulder falls was calculated using the cumulative size frequency distribution (CSFD) of the superimposed craters using the lunar production and chronology functions of Neukum et al. (2001) and Neukum (1983), respectively.

At crater 1, 224 superimposed craters were counted in the diameter range of 3–42 m in an area of 12.09 km^2. The CSFD provides the N (1 km) value of 1.36×10^{-6} km^{-2}, and an absolute model age of 1.62 ± 0.34 Ma. At crater 2, 458 superimposed craters were counted in 3–22 m diameter range in an area of 4.59 km^2. The CSFD gives the N (1 km) value of 1.30×10^{-6} km^{-2} and an absolute model age of 1.55 ± 0.54 Ma. Considering the errors, the boulder falls (set 2) at both craters may be considered to have formed at 1.6 Ma (**Figure S7**). On the other hand, the boulders trails without superimposed craters (first set) should be younger than 1.6 Ma and likely formed during the 3rd January 1975 moonquake. The age of boulders without trails (third set) may not be older than 150-300 Ma, considering the survival times of meter-sized lunar boulders (e.g., Basilevsky et al., 2013).

4.5. Ground Motion Simulations

In this section, we present the results from the ground motion simulations for understanding the conditions that are required for the origin of boulder falls at impact craters 1 and 2, due to the M_W 4.1 moonquake (with 210 MPa stress drop) that occurred either at a focal depth of 1 km or 5 km, along the largest lobate scarp segment (11.3 km segment; **Figure 2b**) in Laue crater. The depth of faulting along the scarp segment may not exceed 5 km, considering 40° fault dip and fault aspect ratio of 2. For the simulations, we have used the stochastic seismological model by Boore (2003) (**Supplementary Materials**). Firstly, synthetic accelerogram is simulated for the Apollo 16 station location for the 3rd January 1975 moonquake and compared with the Apollo 16 recorded data. The Fourier amplitude spectrum of the simulated data is in good agreement with the recorded data in the frequency range of 1Hz to ≈10 Hz (**Figure 4a**). Thereafter, acceleration time histories are simulated around the epicenter up to a radial distance of 80 km for estimating the peak ground acceleration (PGA) (**Figure 4b**). For a focal depth of 1 km, PGA value is 70 g at an epicentral distance of 3 km and it decreases to 0.86 g at 80 km from the epicenter (**Figure 4b**). Similarly, for a focal depth of 5 km, the PGA values are 13.7 g and 0.26 g at 3 km and 80 km respectively (**Figure 4b**). At crater 2 (25 km from the relocated epicenter), the PGA values are 5.5 g and 1.4 g for 1 km and 5 km focal depths, respectively. Likewise, at crater 1 (30 km from the relocated epicenter), the PGA values are 4.4 g and 1.1 g, respectively. These PGA values are strong enough to produce boulder falls at craters 1 and 2 (e.g., Yim et al., 1980; Iyengar and Raghukanth, 2006; Kumar et al., 2019).

In order to understand the rocking (or shaking) behaviour of boulders present on the upper interior walls of impact craters 1 and 2 in response to the ground motion associated with 3rd

January 1975 moonquake, we have followed the method given by Yim et al. (1980) (**Supplementary Materials**). The synthetic accelerograms for the craters 1 and 2, respectively for 1 and 5 km focal depths, are shown in **Figures 4c, 4d, 4g** and **4h**. The rocking behaviour of a boulder depends on its size, aspect ratio and radius of gyration. For our simulations, we assume the boulders have the observed mean size and aspect ratio. In addition, the duration of rocking and point of toppling depend upon the mass moment of inertia of the boulder and the ground motion characteristics. In response to the ground acceleration time history for 1 km focal depth (**Figure 4c**), the boulders at crater 1 would start shaking at a horizontal acceleration of 0.575 g and continue to shake for 0.672 seconds before it eventually topples at 0.522 g (**Figures 4e**). When the focal depth increases to 5 km (**Figure 4d**), the boulder shaking starts at 0.702 g, and shaking continues for a period of 0.67 seconds, before falling at 0.545 g (**Figure 4f**). In response to the ground acceleration time history for 1 km and 5 km focal depths (**Figures 4g** and **4h**), the boulders at crater 2 would start shaking at 0.524 g and 0.608 g, respectively, and shaking continues for 0.67 s before they eventually fall at an acceleration of 1.275 g and 0.543 g respectively (**Figure 4i** and **4j**). Our simulations confirm that the occurrence of M_W 4.1 moonquake along the lobate scarp at a focal depth of 1-5 km range would produce strong ground vibrations that are adequate for toppling the boulders at craters 1 and 2. Hence, we interpret that the boulder falls are of co-seismic origin.

4.6. Impact Triggered Seismicity

Since the shallow moonquake occurred in 1975, we estimate the seismicity from recent impact events in the last 50 years, based on the lunar production and chronology function (Neukum et al., 2001; Neukum, 1983) for calculating the number density of impact craters

that are expected to have formed within the area covering Laue crater (**Supplementary Materials**). In our simulations, twenty nine impact craters in the diameter range of 5-8 m were formed in the last 50 years; one impact crater was formed with 8 m diameter (**Table S2**). The equivalent seismic moment magnitudes of 5, 6, 7 and 8 m impact craters are M_W 1.01, 1.15, 1.26 and 1.36, respectively. These values are significantly lower than that of 3rd January 1975 shallow moonquake that occurred at Laue crater and their seismic ground motion should be weaker than that produced by the moonquake.

5. Discussion and Conclusion

The lobate scarps detected near the 3rd January 1975 moonquake epicenter site is new, considering the global distribution of lobate scarps (Watters et al., 2015). Considering the scarp lengths and their spatial distribution over a long distance, the scarps cannot be just a result of 3rd January 1975 moonquake. Different segments of the lobate scarps may have originally formed episodically over tens to hundreds of million years as in the case of several other lobate scarps globally (e.g., Kumar et al., 2016; Van der Bogert et al., 2018) and they may continue to slip to the present. The NNW-ESE to E-W orientation of lobate scarps is also intriguing, as the orientation of scarps and their locations coincide with the buried Lorentz basin wall beneath Laue crater. As seen in many other peak-ring and multi-ring basins, the Lorentz basin wall represents numerous curvilinear normal faults (e.g., Nahm et al., 2013) and a segment of which is present beneath the Laue crater (**Figure 1**). Hence, origins of the lobate scarps are related to the reverse slips along the Lorentz basin wall normal fault. Episodic reactivation of the basin wall normal fault produced different segments of lobate scarps. The slips along the sub-surface thrust faults are also responsible for the

origins of shallow moonquakes, as seen in lobate scarps present in the Schrödinger basin (e.g., Kumar et al., 2016).

The boulder falls are important indicators of recent seismic shaking of planetary surfaces (e.g., Hovland and Mitchell, 1973; Roberts et al., 2012; Kumar et al., 2013; Kumar et al., 2016; Kumar et al., 2019). Boulders are abundant on the rim and upper wall of impact craters, as they are produced during the host crater formation in response to impact fracturing and spallation processes (e.g., Kumar et al., 2014; Krishna and Kumar, 2016) and these are the sources of boulder falls on the interior walls of craters 1 and 2. On Earth, the co-seismic boulder falls are formed in response to strong earthquake ground motion (e.g., Keefer, 1984). Similarly, the boulder falls in craters 1 and 2 are formed in response to moonquake ground motion that originated from the lobate scarps (**Figure 3**). Our ground motion simulations confirm the possibility that the moonquakes occurring along the lobate scarps can produce strong ground motions capable of triggering boulder avalanches at craters 1 and 2 (**Figure 4**). Hence, the presence of three sets of boulder falls suggest that they were formed at least during three different moonquake events. The youngest boulder fall event is interpreted to be related to the 3rd January 1975 shallow moonquake. The second set of boulders was emplaced during another moonquake event around 1.6 Ma, and the third set formed during a much older event (<150-300 Ma). Impact events are unlikely sources of ground motion at least for triggering the younger boulder falls. Thus, we suggest that the lobate scarps in Laue crater, identified in the present study, are seismically active.

Our finding of seismically active lobate scarps in Laue crater is important considering their link to the instrumentally recorded shallow moonquake and the effects of its ground motion on the formation of co-seismic boulder avalanches. The co-existence of lobate scarps and

distribution of boulder fall sites around them provide a new approach for identifying seismically active zones on the Moon and thereby facilitating moonquake hazard analysis for the future landing missions including human exploration of the Moon.

Acknowledgements

PSK acknowledges Indian Space Research Organization (ISRO) and Council of Scientific and Industrial Research (India) for funding the research, and Tom Watters for providing the global data of lunar lobate scarps. GRL editor Andrew Dombard is thanked for helpful discussions. We appreciate the reviewers Amanda Nahm and Renee Weber for their thoughtful review comments and suggestions that significantly improved the paper. The LRO mission data used in our work are freely available in the NASA PDS and USGS websites; the datasets generated from our geologic analysis and numerical simulations are presented in the form of figures and supplementary materials. V.M. Tiwari, Director, CSIR-NGRI is acknowledged for granting permission to publish this paper (Publication No. NGRI/Lib/2019/Pub-44). RPR acknowledges the Head, PSD and Director, SAC (ISRO).

References

Baker, D. M., et al., (2012). The transition from complex craters to multi-ring basins on the Moon: Quantitative geometric properties from Lunar Reconnaissance Orbiter Lunar Orbiter Laser Altimeter (LOLA) data. *Journal of Geophysical Research: Planets*, *117* (E12). https://doi.org/10.1029/2011je004021

Barker, M. K., et al., (2016). A new lunar digital elevation model from the Lunar Orbiter Laser Altimeter and SELENE Terrain Camera, *Icarus*, 273, 346-355. https://doi.org/10. 1016/ j.icarus. 2015.07.039.

Basilevsky, A. T., et al., (2013). Survival times of meter-sized boulders on the surface of the Moon. *Planetary and Space Science*, *89*, 118-126. https://doi.org/10.1016/j.pss.2013.07.011

Boore, D. M. (2003). Simulation of ground motion using the stochastic method. *Pure and Applied Geophysics*, *160*(3-4), 635-676. https://doi.org/10.1007/PL00012553

Hovland, H. J. and J. K. Mitchell (1973). Boulder tracks and nature of lunar soil. *The Moon*, 6(1-2), 164-175. https://doi.org/10.1007/BF02630660

Howard, K. A. (1973). Avalanche mode of motion: Implications from Lunar examples. *Science*, 180 (4090), 1052-1055. https://doi.org/10.1126/science.180.4090.1052

Iverson, R. M. (1997). The physics of debris flows. *Reviews of Geophysics*, *35*(3), 245-296.

Keefer, D. K., (1984). Landslides caused by earthquakes. Geological Society of America Bulletin, 95(4), 406-421. https://doi.org/10.1130/0016-7606(1984)

Iyengar, R. N., and S. T. G. Raghukanth (2006). Strong ground motion estimation during the Kutch, India earthquake. *Pure and Applied Geophysics*, 163(1), 153-173. https://doi.org/10.1007/s00024-005-0006-x

Kneissl, T., et al., (2011). Map-projection-independent crater size-frequency determination in GIS environments—New software tool for ArcGIS. *Planetary and Space Science*, *59*(11-12), 1243-1254. https://doi.org/10.1016/j.pss.2010.03.015

Krishna, N. and P. S. Kumar, (2016). Impact spallation processes on the Moon: A case study from the size and shape analysis of ejecta boulders and secondary craters of Censorinus crater. *Icarus*, 264, 274-299. https://doi.org/10.1016/j.icarus.2015.09.033

Kumar, P.S., et al., (2013). Gullies and landslides on the Moon: Evidence for dry-granular flows. *Journal of Geophysical Research: Planets*, 118(2), 206-223. https://doi.org/10.1002/jgre.20043

Kumar, P.S., et al., (2014). Impact fragmentation of Lonar Crater, India: Implications for impact cratering processes in basalt. *Journal of Geophysical Research: Planets*, *119*(9), 2029-2059. https://doi.org/10.1002/2013JE004543

Kumar, P.S., et al., (2016). Recent shallow moonquake and impact-triggered boulder falls on the Moon: New insights from the Schrödinger basin. *Journal of Geophysical Research: Planets*, 121(2), 147-179. https://doi.org/10.1002/2015je004850

Kumar, P.S., et al., (2019). Recent seismicity in Valles Marineris, Mars: Insights from young faults, landslides, boulder falls and possible mud volcanoes. *Earth and Planetary Science Letters*, *505*, 51-64. https://doi.org/10.1016/j.epsl.2018.10.008

Michael, G.G. and G. Neukum, (2010). Planetary surface dating from crater size–frequency distribution measurements: Partial resurfacing events and statistical age uncertainty. *Earth and Planetary Science Letters*, 294, 223-229. https://doi.org/10.1016/j.epsl.2009.12.041

Nahm, A.L., et al., (2013). Normal faulting origin for the Cordillera and Outer Rook rings of Orientale Basin, the Moon. *Journal of Geophysical Research: Planets*, *118*(2), 190-205. https://doi.org/10.1002/jgre.20045

Nakamura, Y., (1980). Shallow moonquakes: How they compare with earthquakes. *Proceedings of Lunar and Planetary Science Conference*, *11*, 1847-1853.

Nakamura, Y., et al., (1979). Shallow moonquakes: Depth, distribution and implications as to the present state of the lunar interior. *Proceedings of Lunar and Planetary Science Conference*, 10, 2299-2309.

Neukum, G., (1983). Meteoriten bombardement and Datierung Planetarer Oberflächen, Habilitation Dissertation for Faculty Membership, Univ. of Munich, 186 pp.

Neukum, G., et al., (2001). Cratering records in the inner solar system in relation to the lunar reference system. In *Chronology and evolution of Mars*, 55-86. Springer, Dordrecht. https://doi.org/10.1007/978-94-017-1035-0_3

Neumann, G.A., et al., (2015). Lunar impact basins revealed by Gravity Recovery and Interior Laboratory measurements. *Science Advances*, 1(9), 1500852. https://doi.org/10.1126/sciadv.1500852

Oberst, J., (1987). Unusually high stress drops associated with shallow moonquakes. *Journal of Geophysical Research: Solid Earth*, *92*, 1397-1405. https://doi.org/10.1029/jb092ib02p01397

Roberts, G.P., et al., (2012). Possible evidence of paleomarsquakes from fallen boulder populations, Cerberus Fossae, Mars. *Journal of Geophysical Research: Planets*, 117(E2). https://doi.org/10.1029/2011JE003816

Robinson, M. S., et al., (2010). Lunar reconnaissance orbiter camera (LROC) instrument overview. *Space Science Reviews*, 150(1-4), 81-124. https://doi.org/10.1007/s11214-010-9634-2

Smith, D.E., et al., (2010). Initial observations from the lunar orbiter laser altimeter (LOLA). *Geophysical Research Letters*, 37(18), L18204. https://doi.org/10.1029/2010GL043751

Van Der Bogert, C.H., et al., (2018). How old are lunar lobate scarps? 1. Seismic resetting of crater size-frequency distributions. *Icarus*, 306, 225-242. https://doi.org/10.1016/j.icarus.2018.01.019

Watters, T.R., et al., (2010). Evidence of recent thrust faulting on the Moon revealed by the Lunar Reconnaissance Orbiter Camera. *Science*, 329, 936-940. https://doi.org/10.1126/science.1189590

Watters, T.R., et al., (2015). Global thrust faulting on the Moon and the influence of tidal stresses. *Geology*, 43(10), 851-854. https://doi.org/10.1130/G37120.1

Yim, C.S., et al., (1980). Rocking response of rigid blocks to earthquakes. *Earthquake Engineering and Structural Dynamics*, 8(6), 565-587. https://doi.org/10.1002/eqe.4290080606

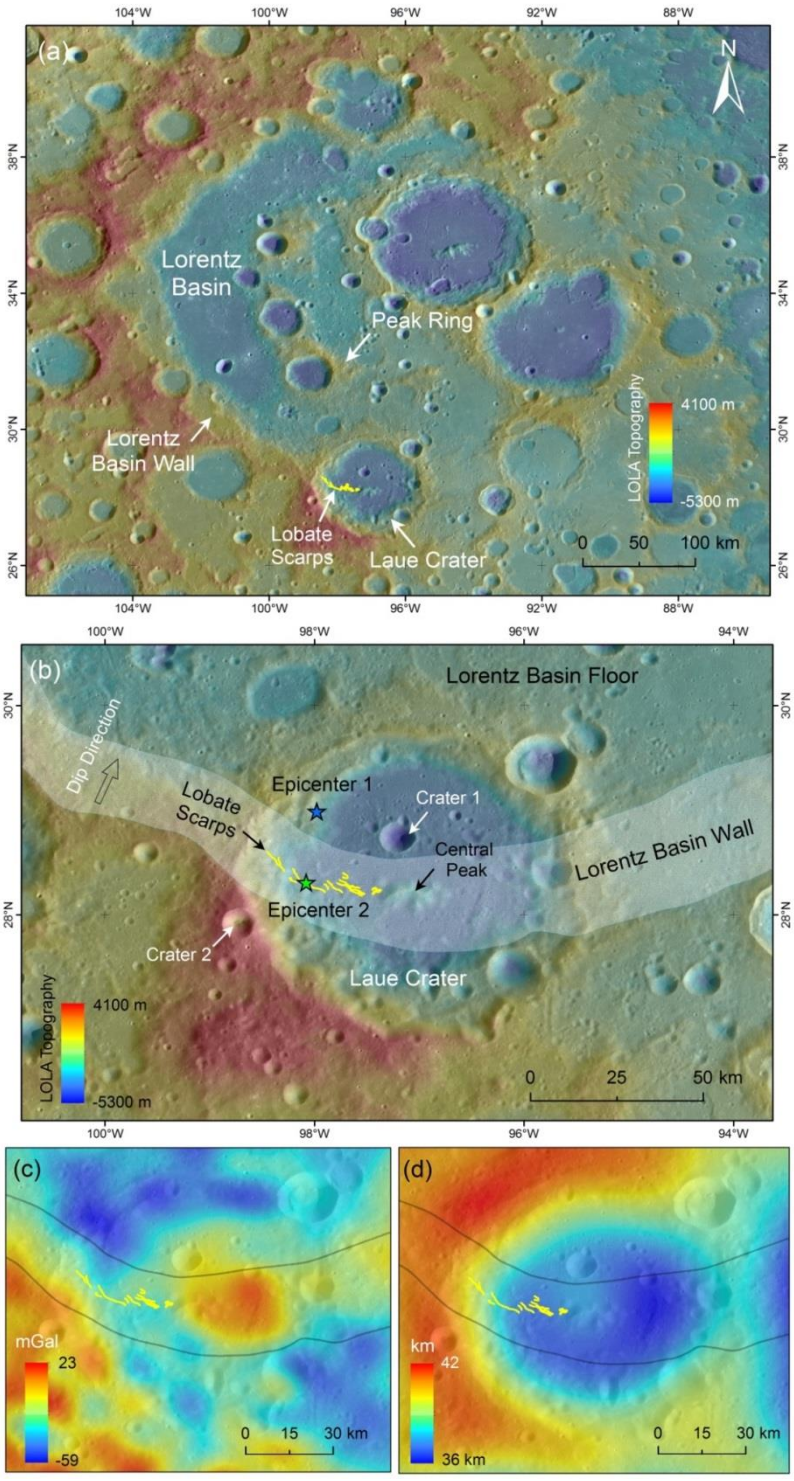

Figure 1: Geology of the study area: LROC WAC image mosaic overlain by LOLA topography showing Lorentz basin (a) and Laue crater (b); (c) residual Bouguer gravity anomaly (GRAIL) and (d) crustal thickness maps of the Laue crater region. The locations of lobate scarps (yellow lines shown in a-d) coincide with the Lorentz basin wall. Impact craters 1 and 2 (shown in b) exhibit boulder falls on their interior walls. The epicenter of 3rd January 1975 (M_W 4.1) shallow moonquake (epicenter 1) has been relocated to the longest segment of the lobate scarps (epicenter 2) mapped in the study.

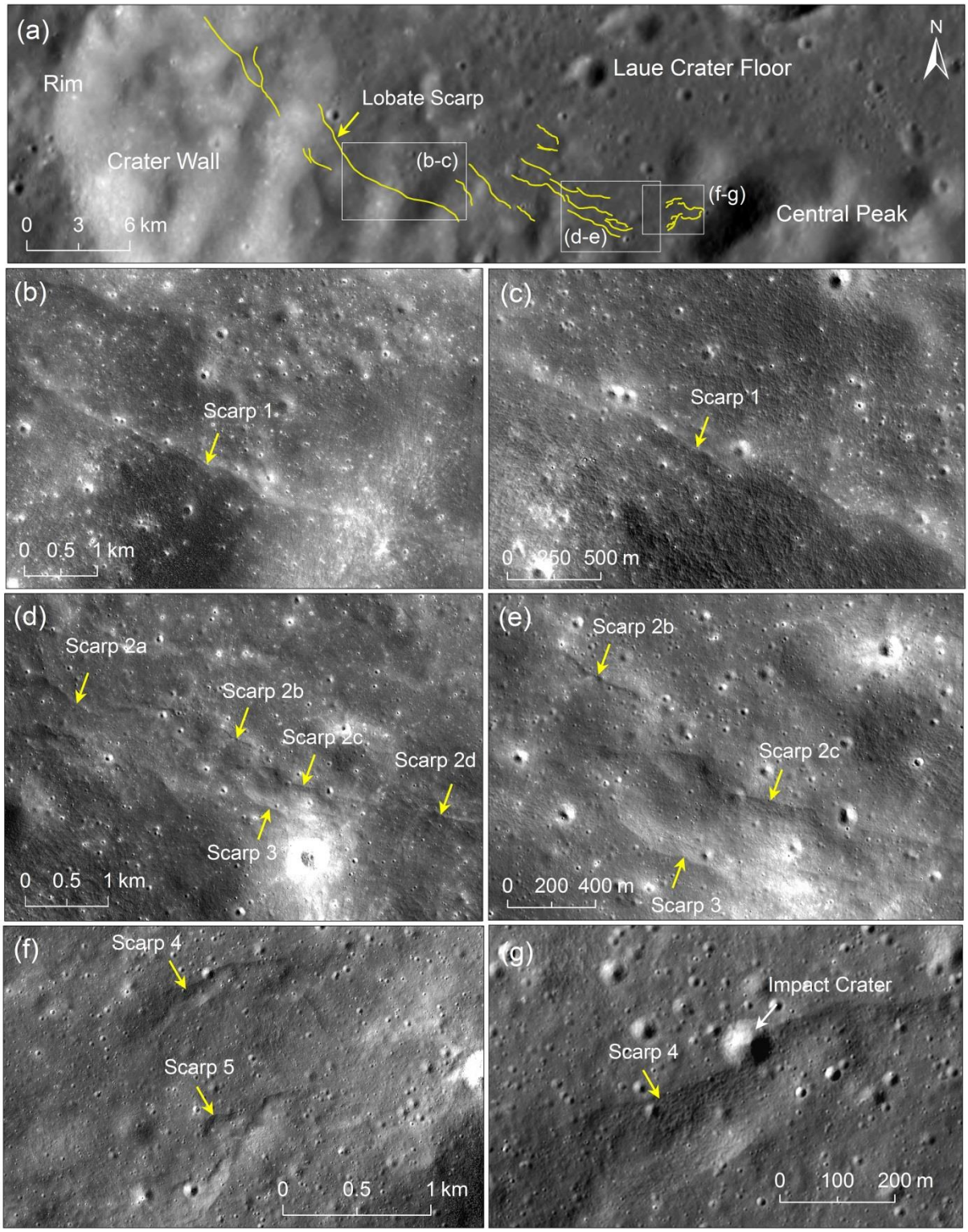

Figure 2: The newly identified lobate scarps: (a) LROC WAC image mosaic showing the lobate scarps (yellow lines) occurring on the Laue crater floor. (b) and (c): LROC NAC (M1145447946RE and M105155992LE) images showing the longest segment of the lobate scarps occurring on the western side; (d) and (e): LROC NAC (M105155992RE) images showing the lobate scarps in the central part; (f) and (g) LROC NAC (M1106552598RE) images showing the lobate scarps in the eastern side.

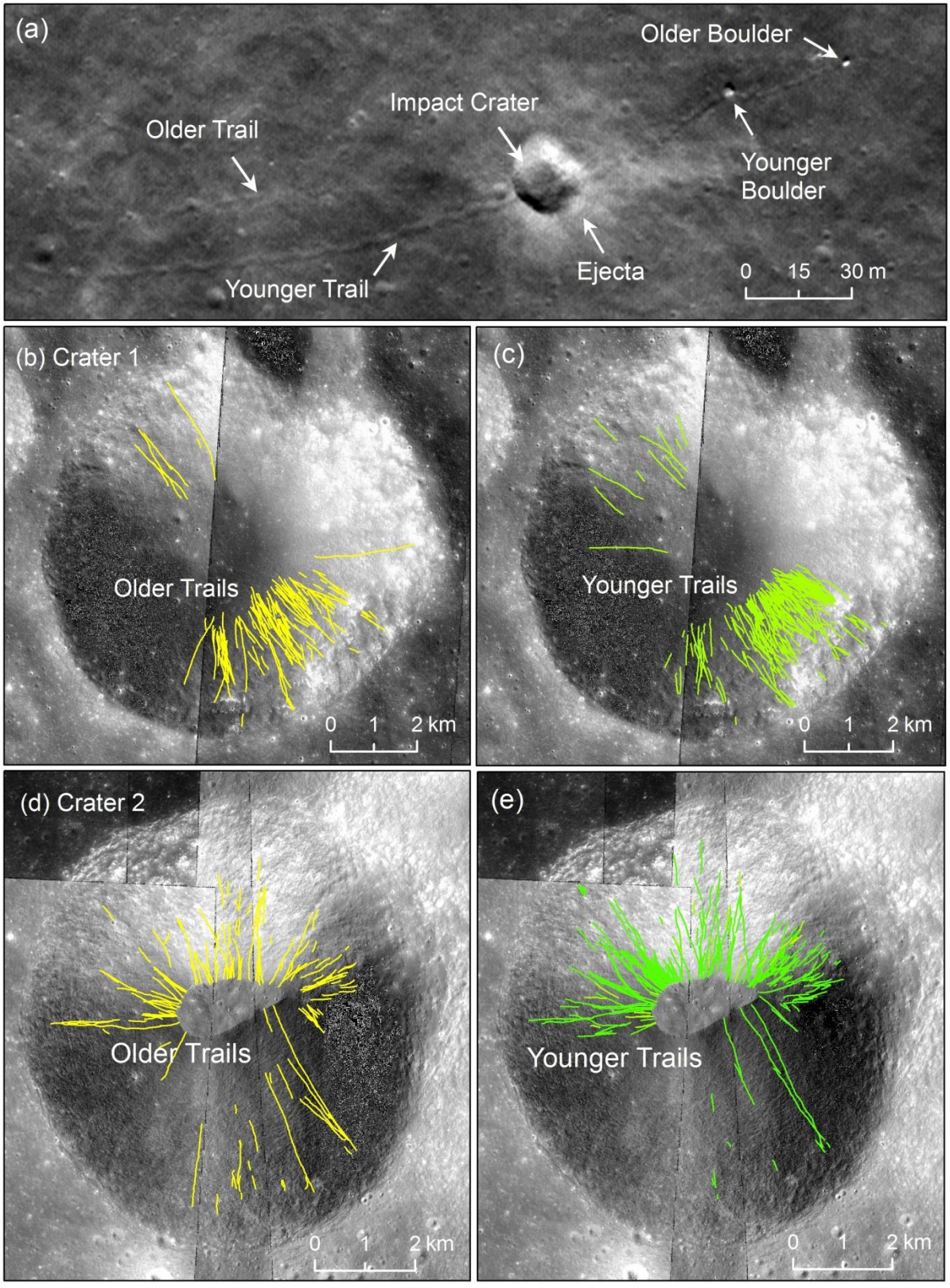

Figure 3: The boulder avalanches at craters 1 and 2: (a) LROC NAC image (M155886005LE) showing the boulder falls of two different formation times: the older trail is superimposed by an impact crater, while the young trail cross-cuts the impact crater. (b-d) and (c-e) older and younger boulder trails of craters 1 and 2, respectively. LROC NAC images M1206659832LE and M1206659832RE are used in (b-c) and M1114824689RE, M1106559741RE, M160601439RE, M155886005RE and M155886005LE in (d-e).

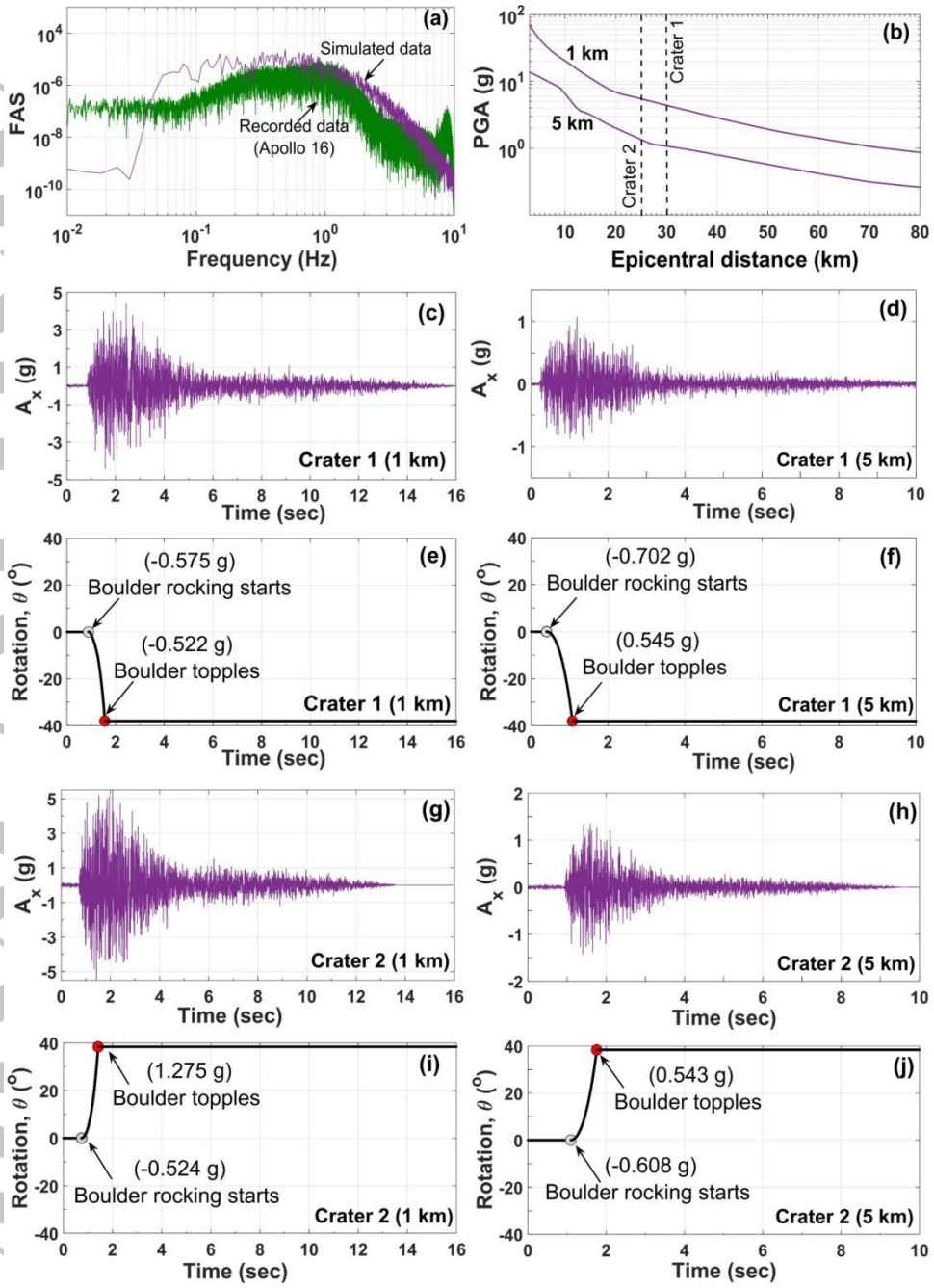

Figure 4: The seismic ground motion models: (a) Fourier amplitude spectrum (FAS) of simulated and recorded vertical components of accelerograms for 3rd January 1975 moonquake at Apollo 16 seismic station. (b) Variation of horizontal peak ground acceleration (A_X) in terms of lunar gravity (g = 1.62 m/s^2) with increasing radial distance (3-80 km) from 9th January 1975 (M_W 4.1) moonquake epicenter, for 1 km and 5 km focal depths. (c and d) Simulated horizontal accelerograms for crater 1, respectively for focal depths 1 km and 5 km. (e and f) Rocking behaviour of an average sized boulder at crater 1, when subjected to the ground motions as in (c) and (d) respectively. (g and h) Simulated horizontal accelerograms for crater 2, for focal depths 1 km and 5 km respectively, and the rocking response of boulders located at crater 2 are shown in (i) and (j).